Ultrafast electron cascades in semiconductors driven by intense femtosecond terahertz pulses

H. Wen,[1] M. Wiczer,[3] and A. M. Lindenberg[1,2]
[1]*PULSE Institute, Stanford Linear Accelerator Center, Menlo Park, California 94025, USA*
[2]*Department of Materials Science and Engineering, Stanford University, Stanford, California 94305, USA*
[3]*Department of Physics, University of Illinois at Urbana-Champaign, Urbana, Illinois 61801, USA*
(Received 10 August 2008; published 10 September 2008)

An ultrafast terahertz (THz) source has been employed to study the nonlinear response of semiconductors to near-half-cycle femtosecond pulses in the THz regime. We report nonlinear absorption and self-phase modulation of the THz pulses associated with ultrafast impact ionization processes and the development of an electron cascade on femtosecond time scales by THz pump–THz probe measurements.

DOI: 10.1103/PhysRevB.78.125203 PACS number(s): 78.47.Fg, 42.65.Re, 78.40.Fy

I. INTRODUCTION

Intense terahertz (THz) radiation provides a new means of controlling material properties through manipulation of charge carriers, dipoles, or vibrational degrees of freedom, with applications to all-optical switching technology, THz-biased devices, and materials processing. With wavelengths in the far infrared, near– half-cycle THz pulses can be thought of as ultrafast electric or magnetic-field pulses which turn on and off on times orders of magnitude faster than that achieved through standard electronics. Although THz radiation has been widely used as a noncontact probe of sample properties, the interaction of intense far-infrared pulses with matter is just beginning to be explored.[1–5] New sources of ultrashort high-field pulses have been developed in both the laboratory[6,7] and at accelerator-based settings,[8,9] providing unique opportunities to investigate and direct the properties of materials under high-field conditions.

Intense THz pulses typically interact with materials through three basic mechanisms. With photon energies of a few meV, THz fields may resonantly drive vibrational or electronic states in molecules, nanostructures, and bulk solids. The nonlinear responses of these excitations reveal, for instance, lattice vibrational anharmonicity[3] and the dynamics of excitonic polarization.[4] Alternatively, there exist nonresonant excitation mechanisms at high intensities, in analogy to the optical excitation and breakdown phenomena observed in transparent materials under intense optical fields.[10,11] For example, the large ponderomotive energies associated with high-field THz pulses (proportional to λ^2) can modify the interatomic potential such that electrons tunnel into the continuum with high probability.[12–15] Finally, free carriers can be accelerated in THz fields, leading to free-carrier absorption and, in the limit of high THz fields, the development of impact ionization processes,[16–19] in which a cascade of secondary electron generation occurs in the applied field.[20–22] In this paper we study THz nonlinear absorption and self-phase modulation (SPM) associated with impact ionization processes induced by intense femtosecond THz fields. By THz pump–THz probe measurements, we time resolve the electron-electron scattering and ionization processes, corresponding to real-time measurement of the first steps in the optical breakdown of transparent materials.

II. THz NONLINEAR ABSORPTION IN InSb

We employ a z-scan technique to study the nonlinear THz transmission through undoped indium antimonide (InSb) samples. High–field THz pulses are generated using a setup (Fig. 1) similar to that described in Refs. 7 and 23–25. A 0.8 mJ, 800 nm, 50 fs pulse is focused by a $f=200$ mm lens through a 100 μm type-I beta-barium borate (BBO) crystal, generating a plasma through ionization of the air, which acts as a nonlinear medium for THz generation by mixing of the fundamental and second harmonic.[26] The collinear emitted 300 fs THz pulse [Fig. 2(a)] is selected out by a crystalline silicon filter and is collected, collimated, and refocused by a pair of 90° off-axis parabolic mirrors onto a 390 μm thick, 111-cut InSb wafer. The sample is mounted normally to the THz pulse in a temperature controlled cryostat with polypropylene windows. By scanning the sample through the focus of the THz pulse [Fig. 2(b), inset] while monitoring the transmitted beam, we directly map out the field-dependent transmission characteristics. The transmitted pulse is then recollected onto a liquid-helium-cooled Si bolometer or measured directly using an electro-optic (EO) sampling technique.[27] As shown in Fig. 3(a), we observe a dramatic suppression of the THz transmission near the focus, corresponding to the development of nonlinear THz absorption at high fields. Figure 3(b) shows the extracted absorption coefficient as a function of the peak field of the THz pulse, which

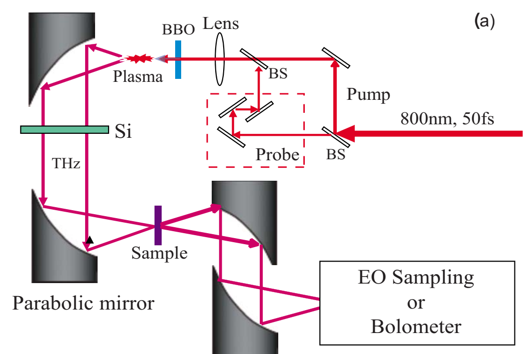

FIG. 1. (Color online) The experimental setup. The dashed box represents the probe channel that is used in THz pump–THz probe measurements. BS: beam splitter; Si: silicon wafer; BBO: beta-barium borate crystal.

 ©2008 The American Physical Society

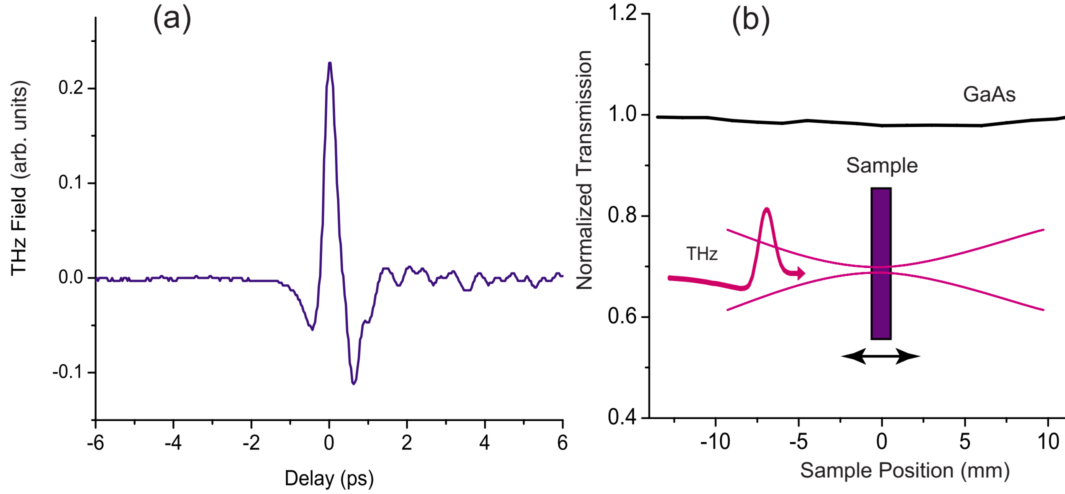

FIG. 2. (Color online) (a) A typical THz field wave form detected by an electro-optical sampling technique. (b) The normalized THz transmission for GaAs as a function of sample position at room temperature. The inset shows the layout of the z-scan technique.

is calibrated using electro-optical sampling. The data points within the Rayleigh range [$z=-2.5$ to 2.5 mm, inset, Fig. 3(b)] are not included in order to avoid complications associated with interference effects[28] and the Gouy phase shift,[29,30] near the focus. These nonlinear absorption effects are not observed in larger band-gap materials such as gallium arsenide [GaAs, Fig. 2(b)] or silicon.

Far from the focus, in the linear absorption region, the dominant THz absorption mechanism is free-carrier absorption from thermally-excited carriers. Other absorption mechanisms are negligible because the THz photon energies lie far below the band gap or lattice absorption modes[31] (the band gap of InSb is roughly 56 times larger than the energy of a 1 THz photon). The transmittance of the incident THz pulse in this region can then be calculated using a Drude model,[32] in which the complex frequency-dependent dielectric function $\epsilon(\omega)$,

$$\epsilon(\omega) = \epsilon_\infty \left(1 - \frac{\omega_p^2}{\omega^2 + \tau^{-2}} + i \frac{\omega_p^2 \tau^{-1}}{\omega(\omega^2 + \tau^{-2})} \right), \tag{1}$$

is related to the free-carrier density N by the plasma frequency $\omega_p = \sqrt{Ne^2/\epsilon_\infty \epsilon_0 m_e^*}$, where m_e^* is the effective electron mass, e is the electron charge, ϵ_0 and ϵ_∞ are the dielectric constant and the relative dielectric constant for infinite frequencies, respectively, and τ is the electron-scattering time constant. The contribution of holes is negligible as the heavy-hole effective mass in InSb is 29 times larger than that of the electrons. Since the plasma frequency ω_p lies within the THz spectrum, the transmittance is sensitive to changes in the free-carrier concentration. At 77 K, the free-carrier concentration of the sample is 1.1×10^{14} cm^{-3}, corresponding to $\omega_p / 2\pi = 0.2$ THz. From $\epsilon(\omega)$, we can calculate the THz transmission including losses from both reflection and sample absorption. The THz transmission as a function of the sample temperature [circles, Fig. 4(a)] in this region agrees well with the Drude model calculation [solid line, Fig. 4(a)]. As the sample is moved closer to the THz focus (the nonlinear absorption region), the drop in transmission can then be

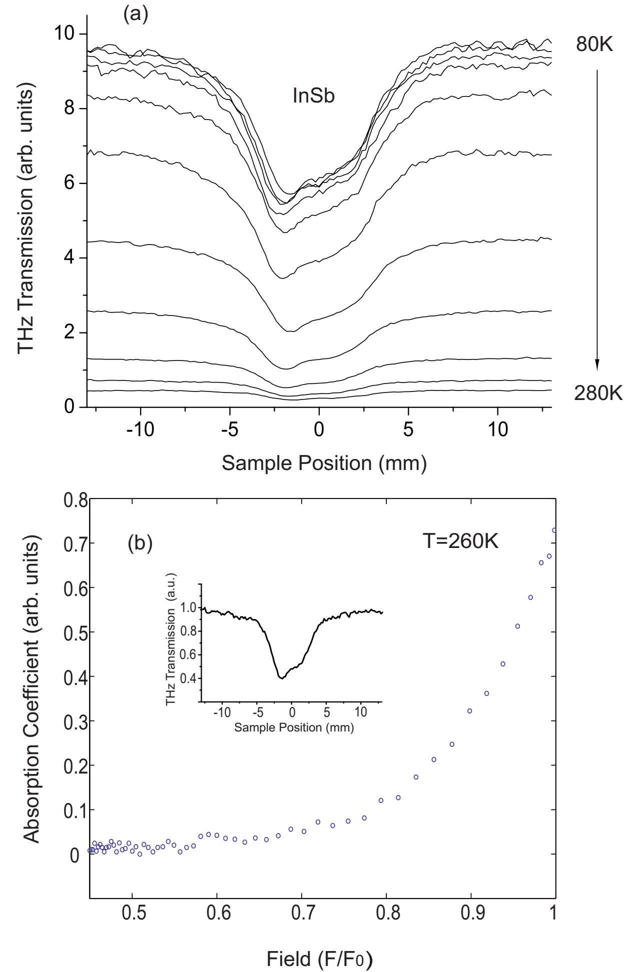

FIG. 3. (Color online) (a) The THz transmission for an InSb sample as a function of position at various temperatures from 80 to 280 K with 20 K intervals. (b) The THz absorption coefficient as a function of the peak THz field (normalized to the maximum peak field F_0 at the focus) at $T=260$ K. The inset shows the corresponding z scan.

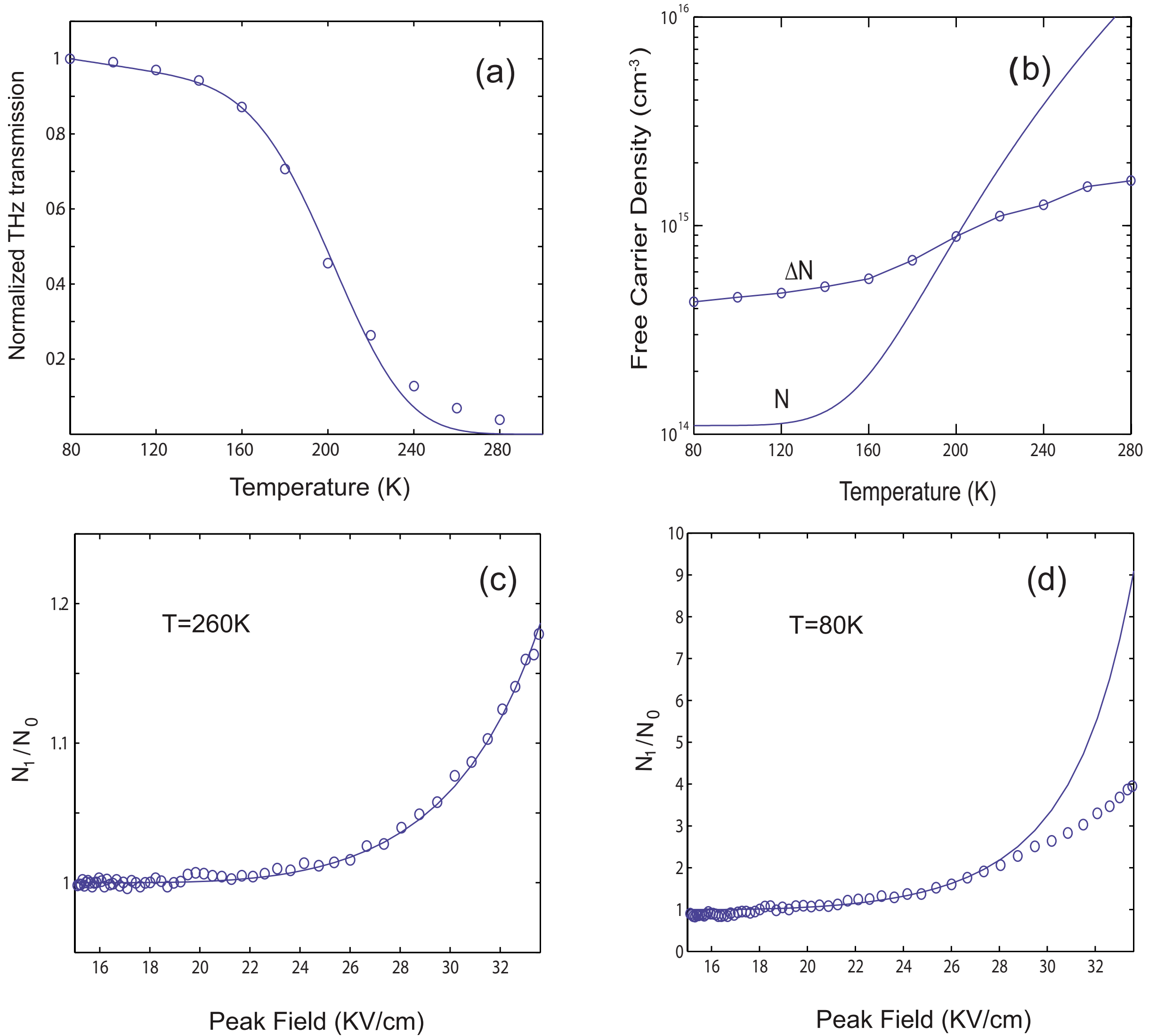

FIG. 4. (Color online) (a) The measured (circle) and calculated (solid line) THz transmission as functions of the sample temperature in the linear absorption region, normalized to the transmission at 80 K. (b) The change in the free-carrier density (circles) and the calculated background free-carrier density (solid line) as functions of the temperature. (c) The free carrier density (N_1) after the THz pulse over that (N_0) before the pulse as functions of the peak field at $T=260$ K (circle: measured; solid line: calculated). d) Same as c) except at $T=80$ K.

understood as a result of the generation of free carriers by the THz pulse. This may occur through impact ionization processes driven by the leading edge of the THz pulse and subsequent free-carrier absorption by the trailing edge along with the following small amplitude oscillation of the THz waveform. The validity of this model is checked in four different ways: (1) Measurement of the temperature dependence of the observed nonlinearity; (2) Comparison of observed data to models of the impact ionization process in the THz field; (3) THz pump–THz probe measurements with independent pump and probe beams; and (4) electro-optic sampling measurements of the induced pulse reshaping associated with free-carrier generation during the THz pulse.

From the temperature dependent z scans, the THz-induced change in free-carrier concentration (ΔN) can be simply estimated by measuring the change in transmission, under the zeroth order approximation that the entire THz waveform experiences the absorption of the newly generated free carriers. As a function of temperature, it is shown in Fig. 4(b) that the absolute change of the free carrier density (circles) increases with temperature, or equivalently, with the base free-carrier density (solid line), as expected from a field-induced impact ionization model. The strong dependence on the existing, thermally populated free-carrier concentration supports the interpretation that thermally-generated free carriers act as a seed for the carrier generation process. These results also indicate that Franz-Keldysh tunneling ionization[12–15] and multiphoton excitation[33] are not the dominant mechanism for free-carrier generation, since one would not expect a strong dependence on the background free-carrier population. We note that while ΔN increases with temperature, the normalized change $\Delta N/N$ decreases as a function of temperature. This follows as a result of the reduction in the average applied field at high temperatures due

to free-carrier absorption, giving rise to a depth-dependent field inhomogeneity.

III. MODELING: ULTRAFAST ELECTRON CASCADES

The THz-induced time-dependent free-carrier density $N(t)$ can be calculated from the rate equation

$$\frac{dN(t)}{dt} = N(t)\int_{-\infty}^{\infty} f(E,t)\varpi(E)dE, \tag{2}$$

where ϖ is the impact ionization rate and $f(E,t)$ is the energy distribution function of the conduction-band electrons. Electron-hole recombination has been ignored since the THz pulse duration is much shorter than the recombination time.[34] We further approximate the conduction-band electron energy E as that given by the ballistic energy gain E_b of a free electron in the THz field, i.e., $f(E,t) \approx \delta(E-E_b)$, where $E_b(z,t) = (\int_0^t eF(z,t')dt')^2/(2m_e^*)$. Including the fact that the THz field $F(z,t)$ is depth dependent as a result of free-carrier screening, Eq. (2) takes the form $dN(z,t)/dt = N(z,t)\varpi[E_b(z,t)]$. After averaging over the sample thickness d, the solution of Eq. (2) is

$$N(t) = \frac{N(0)}{d}\int_0^d e^{\int_0^t \varpi(z,t')dt'} dz. \tag{3}$$

We use the formula given in Ref. 35 to calculate the impact ionization rate of InSb, $\varpi(z,t) = C[E(z,t)-E_i]^2\theta[E(z,t)-E_i]$, where $C \approx 7\times 10^{50}$ $\mathrm{J^{-2}\,s^{-1}}$, E_i is the ionization threshold field, and $\theta(x)$ is the Heaviside function. If the ionization rate is a constant, the solution simplifies to the case of impact ionization in a dc electric field, $N(t) = N(0)e^{\varpi t}$, as expected. Using these equations, the data taken at 260 K in Fig. 4(c) are well fit with just one adjustable parameter, the THz peak field. Best fit corresponds to a peak field of 33.6 kV/cm at the focus in good agreement with that estimated by the electro-optic sampling technique (32 kV/cm). Therefore, the delta function approximation of the electron energy distribution provides a simple but intuitive model that well describes the weakly nonlinear interaction case, in which the impact ionization probability within the THz pulse envelope is much less than one. This approximation also can be interpreted as a short-pulse approximation in which the THz pulse duration is short compared to the impact ionization time. In contrast, a deviation of the experimental data from the calculation is evident at low temperatures [Fig. 4(d)], where the reduced field screening and reflection lead to higher average fields within the sample. In this case, the approximation breaks down, i.e., a significant number of impact ionization events occur within the THz pulse so that the delta function cannot represent the electron energy distribution accurately.

IV. THz PUMP–THz PROBE MEASUREMENT

To further investigate the impact ionization dynamics, we conducted a THz pump–THz probe experiment using a 10 Hz Ti:sapphire laser system. A Mach-Zehnder interferometer is added before the lens to form pump and probe channels (Fig. 1). Two time delayed 800 nm laser pulses then collinearly propagate through the same focusing lens and BBO crystal to generate pump and probe THz fields whose amplitudes are estimated about 32 and 20 kV/cm, respectively. After transmitting through the InSb sample at 80 K, the peak field of the probe THz pulse is monitored by the EO sampling technique as a function of the delay between the pump and probe. To exclude the effects associated with optical interference in the BBO crystal and field screening in the plasma,[36] the on-focus scan is subtracted from the off-focus scan to obtain the changes induced by intense THz fields only. Figure 5 shows that the peak field of the probe THz pulse is reduced by 25% within 1 ps as a result of absorption in the free carriers generated by the pump THz pulses. The field amplitude reduction is slightly larger than the prediction (21%) from the intensity change in the z-scan measurements. It can be attributed to the fact that the leading edge of the THz pulse does not contribute to the nonlinear absorption in single pulse z-scan measurements. The time resolution in this pump-probe study is limited by the convolution of the duration of pump and probe THz pulses. Nevertheless, the results show that the observed THz-induced impact ionization occurs in less than 1 ps.

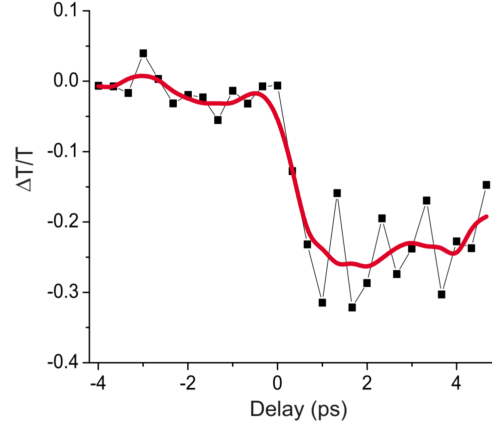

FIG. 5. (Color online) The change of probe THz peak field as a function of the delay between pump and probe THz pulses. The red curve shows three-point adjacent average.

V. THz SELF-PHASE MODULATION

In order to resolve the carrier generation process occurring within the THz waveform, we employed a single intense THz pulse as a pump (leading edge) and probe (trailing edge) simultaneously. The waveforms of the transmitted THz field (Fig. 6) are recorded after the sample (180 K) at a fixed position by an electro-optic sampling technique when the sample is on ($z=-2.5$ mm) and off ($z=-12$ mm) the focus, corresponding to the high- and low-field conditions, respectively. The time resolution of this measurement is limited by the duration of the probe-laser pulse and the bandwidth of the electro-optic crystal. In addition to the amplitude reduction due to nonlinear absorption, we observe a field-dependent phase shift and pulse broadening arising due to the generation of free carriers. The newly generated free carriers act back on the propagating THz pulse and cause

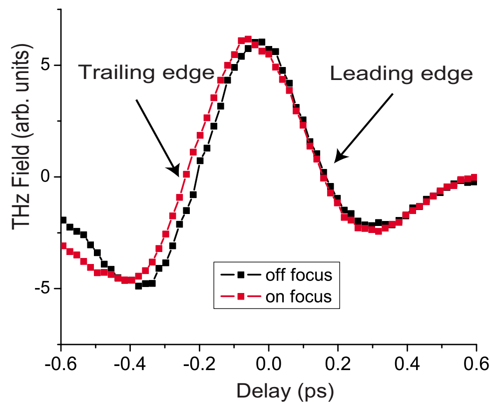

FIG. 6. (Color online) The transmitted single pulse THz waveform at 180 K. The black and red curves are measured when the sample is far from the focus and at the focus, respectively. The amplitudes of the waveforms have been scaled vertically in order to elucidate the field-dependent phase changes.

31 ± 5 fs delay at the trailing edge of the pulse. This constitutes the direct observation of self-phase modulation in the THz regime,[5] in analogy to the self-phase modulation experienced by optical pulses propagating in nonlinear media. This effect is not equivalent to the nonlinear cross-phase modulation observed in the interaction of intense THz fields with optical pulses,[9] since the THz nonlinearity originates in the impact ionization process as opposed to the Pockels effect. The emergence of the phase shift at the trailing edge of the THz waveform vividly captures the development of the electron cascade within the THz field.

VI. CONCLUSION

In conclusion, we have observed THz nonlinear absorption and self-phase modulation associated with impact ionization processes driven by high-field THz pulses in semiconductors. The ability to generate THz fields large enough to induce strong nonlinearities enables opportunities in photonics and all-optical switching, in which ultrafast fields are used to control and direct charge-carrier dynamics in devices. This work provides a means of studying optically-induced breakdown of materials, a process fundamental to laser-based micromachining or surgery, using controllable and known time-dependent field pulses. It also forms the basis for the development of THz-biased avalanche photodiodes, representing single-photon sensitive detectors with high quantum efficiency and femtosecond resolution, gated by the THz pulse envelope.

ACKNOWLEDGMENTS

This work is supported by the Department of Energy, Basic Energy Sciences, through the Stanford PULSE (Photon Ultrafast Laser Science and Engineering) Institute. We thank R.W. Falcone for initial discussions related to this work and R. W. Schoenlein for the use of his bolometer.

[1] P. Gaal, K. Reimann, M. Woerner, T. Elsaesser, R. Hey, and K. H. Ploog, Phys. Rev. Lett. **96**, 187402 (2006).
[2] P. Gaal, W. Kuehn, K. Reimann, M. Woerner, T. Elsaesser, and R. Hey, Nature (London) **450**, 1210 (2007).
[3] T. Hornung, K. Yeh, and K. A. Nelson, *Ultrafast Phenomena XV* (Springer-Verlag, Berlin, 2007).
[4] J. R. Danielson, Y. S. Lee, J. P. Prineas, J. T. Steiner, M. Kira, and S. W. Koch, Phys. Rev. Lett. **99**, 237401 (2007).
[5] J. Hebling, K. Yeh, M. C. Hoffmann, and K. A. Nelson, IEEE J. Sel. Top. Quantum Electron. **14**, 345 (2008).
[6] K. L. Yeh, M. C. Hoffmann, J. Hebling, and K. Nelson, Appl. Phys. Lett. **90**, 171121 (2007).
[7] T. Bartel, P. Gaal, K. Reimann, M. Woerner, and T. Elsaesser, Opt. Lett. **30**, 2805 (2005).
[8] G. M. H. Knippels, X. Yan, A. M. MacLeod, W. A. Gillespie, M. Yasumoto, D. Oepts, and A. F. G. van der Meer, Phys. Rev. Lett. **83**, 1578 (1999).
[9] Y. Shen, T. Watanabe, D. A. Arena, C. C. Kao, J. B. Murphy, T. Y. Tsang, X. J. Wang, and G. L. Carr, Phys. Rev. Lett. **99**, 043901 (2007).
[10] B. C. Stuart, M. D. Feit, S. Herman, A. M. Rubenchik, B. W. Shore, and M. D. Perry, Phys. Rev. B **53**, 1749 (1996).
[11] A. C. Tien, S. Backus, H. Kapteyn, M. Murnane, and G. Mourou, Phys. Rev. Lett. **82**, 3883 (1999).
[12] K. B. Nordstrom, K. Johnsen, S. J. Allen, A. P. Jauho, B. Birnir, J. Kono, T. Noda, H. Akiyama, and H. Sakaki, Phys. Rev. Lett. **81**, 457 (1998).
[13] A. Srivastava, R. Srivastava, J. Wang, and J. Kono, Phys. Rev. Lett. **93**, 157401 (2004).
[14] A. H. Chin, J. M. Bakker, and J. Kono, Phys. Rev. Lett. **85**, 3293 (2000).
[15] S. D. Ganichev, E. Ziemann, T. Gleim, W. Prettl, I. N. Yassievich, V. I. Perel, I. Wilke, and E. E. Haller, Phys. Rev. Lett. **80**, 2409 (1998).
[16] P. A. Wolff, Phys. Rev. **95**, 1415 (1954).
[17] W. Shockley, Solid-State Electron. **2**, 35 (1961).
[18] E. O. Kane, Phys. Rev. **159**, 624 (1967).
[19] G. A. Baraff, Phys. Rev. **128**, 2507 (1962).
[20] A. G. Markelz, N. G. Asmar, B. Brar, and E. G. Gwinn, Appl. Phys. Lett. **69**, 3975 (1996).
[21] S. D. Ganichev, J. Diener, and W. Prettl, Appl. Phys. Lett. **64**, 1977 (1994).
[22] M. C. Hoffmann, J. Hebling, H. Y. Hwang, K. L. Yeh, and K. Nelson, Proceedings of the XVI International Conference on Ultrafast Phenomena, 2008 (unpublished).
[23] D. J. Cook and R. M. Hochstrasser, Opt. Lett. **25**, 1210 (2000).
[24] M. Kress, T. Loffler, S. Eden, M. Thomson, and H. G. Roskos, Opt. Lett. **29**, 1120 (2004).
[25] K. Y. Kim, J. H. Glownia, A. J. Taylor, and G. Rodriguez, Opt. Express **15**, 4577 (2007).
[26] X. Xie, J. Dai, and X.-C. Zhang, Phys. Rev. Lett. **96**, 075005 (2006).
[27] Q. Wu and X. C. Zhang, Appl. Phys. Lett. **67**, 3523 (1995).

[28] H. Zhong, N. Karpowicz, and X.-C. Zhang, Appl. Phys. Lett. **88**, 261103 (2006).
[29] D. You and P. H. Bucksbaum, J. Opt. Soc. Am. B **14**, 1651 (1997).
[30] S. Feng, H. G. Winful, and R. W. Hellwarth, Opt. Lett. **23**, 385 (1998).
[31] H. Y. Fan, Rep. Prog. Phys. **19**, 107 (1956).
[32] C. Kittel, *Solid State Physics* (Wiley, New York, 1976).
[33] A. J. A. Miller, J. Dempsey, J. Smith, C. R. Ridgeon, and G. D. Holah, J. Phys. C **12**, 4839 (1979).
[34] R. D. Grober, H. D. Drew, G. L. Burdge, and B. S. Bennett, J. Appl. Phys. **71**, 5140 (1992).
[35] J. T. Devreese and R. G. van Welzenis, Appl. Phys. A: Solids Surf. **29**, 125 (1982).
[36] X. Xie, J. Xu, J. Dai, and X.-C. Zhang, Appl. Phys. Lett. **90**, 141104 (2007).